Ultrafast Electron Diffraction: Structural Dynamics of the Elimination Reaction of Acetylacetone

Shoujun Xu, Sang Tae Park, Jonathan S. Feenstra, Ramesh Srinivasan, and Ahmed H. Zewail*

Laboratory for Molecular Sciences, Arthur Amos Noyes Laboratory of Chemical Physics, California Institute of Technology, Pasadena, California 91125

Received: May 19, 2004

Ultrafast electron diffraction is reported for the elimination reaction of acetylacetone. For this multipath reaction, upon 266 nm excitation, it is revealed that the major reaction channel is fragmentation from the β carbon, producing OH and 3-penten-2-on-4-yl radicals, with a time constant of 247 ± 34 ps. We determine the structures involved and the changes in bond lengths. These structure-dynamics correlations in different states provide a mechanistic description of the complex reaction landscape.

I. Introduction

In reactions involving conjugated hydrogen-bonded structures, the effects of electron delocalization and resonance can lead to multiple pathways which are determined by the nature of the initial structure(s) involved. This complexity is common, particularly for enolones, the enol tautomers of β-diketones. In addition to the initial structures of the keto and enol tautomers, the enol itself may, in principle, exist as an asymmetric (C_s) or symmetric (C_{2v}) structure. The two termini of the conjugated skeleton are connected by an intramolecular hydrogen bond and the asymmetric structures may interconvert via hydrogen shift between the two oxygen atoms. Hence, the thermal and photochemical reactions can be fully described only if all nuclear positions are revealed in the course of the change.

Malonaldehyde and acetylacetone (AcAc) are prototypical β-diketones. In ground-state AcAc, the so-called "resonance-assisted hydrogen bond" has been invoked to define a hybrid symmetric structure,[1,2] but because of the supposedly strong nature of the hydrogen bond, a controversy in the literature resulted in many publications addressing the question − Is the structure of the enol symmetric (C_{2v}) with the hydrogen equally shared by both oxygen atoms, or is it asymmetric (C_s) with the hydrogen localized on only one? Recently, using ultrafast electron diffraction (UED), the ground-state structure of AcAc was shown to be of C_s symmetry.[3]

While the nature of the ground-state structure is now resolved, less is known about the excited states and their reactions. The ultraviolet spectrum of vapor phase AcAc shows a broad structureless absorption which peaks at ∼266 nm and is assigned to the first $\pi\pi^*$ transition (S_2 state) of the enol tautomer.[4,5] The photochemistry has been studied spectroscopically in matrices,[6−8] solutions,[9] and in the gas phase.[10−12] Whereas spectroscopic techniques rely on selectivity to monitor state dynamics, UED resolves the ultrafast structural dynamics of the reaction, as demonstrated earlier for thermal, fragmentation, and ring opening reactions (for review see ref 13).

SCHEME 1: Tautomerization in Enolones

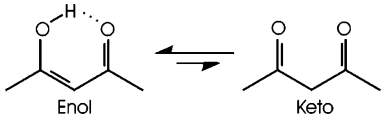

SCHEME 2: Interconversion of the Enol through Hydrogen Shift

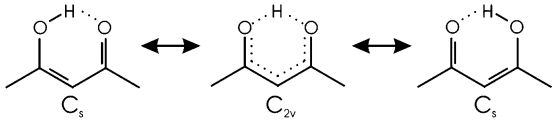

In this article, we report the structural dynamics of isolated, gas-phase AcAc upon 266 nm excitation using UED. The possible reaction pathways are:

SCHEME 3: Possible Reaction Pathways of Acetylacetone

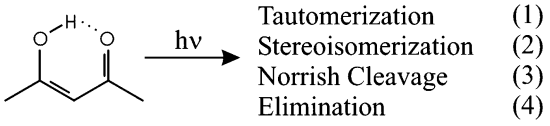

We elucidated the dominance of pathway (4), the structure of the resulting OH elimination product, and the relevant time scale.

II. Experimental Section

The details of our third generation UED apparatus have been reported elsewhere.[13,14] Briefly, the output from an amplified Ti:sapphire laser system (800 nm, 140 fs, 1 kHz) was frequency tripled and split into two beams. The more powerful beam (∼24 μJ) was directed into the scattering chamber to initiate the reaction at 266 nm. The weaker beam (<1 μJ) was time-delayed and focused onto a back-illuminated silver photocathode to generate electron pulses via the photoelectric effect (30 kV; $\lambda_{\text{de Broglie}} = 0.067$ Å). In this study we used ∼18 000 electrons per pulse (width ∼2 ps); for shorter pulses see refs 15 and 16. Electrons were focused by a magnetic lens and directed into

* To whom correspondence should be addressed. E-mail: zewail@caltech.edu.

10.1021/jp0403689 CCC: $27.50
Published on Web 07/17/2004

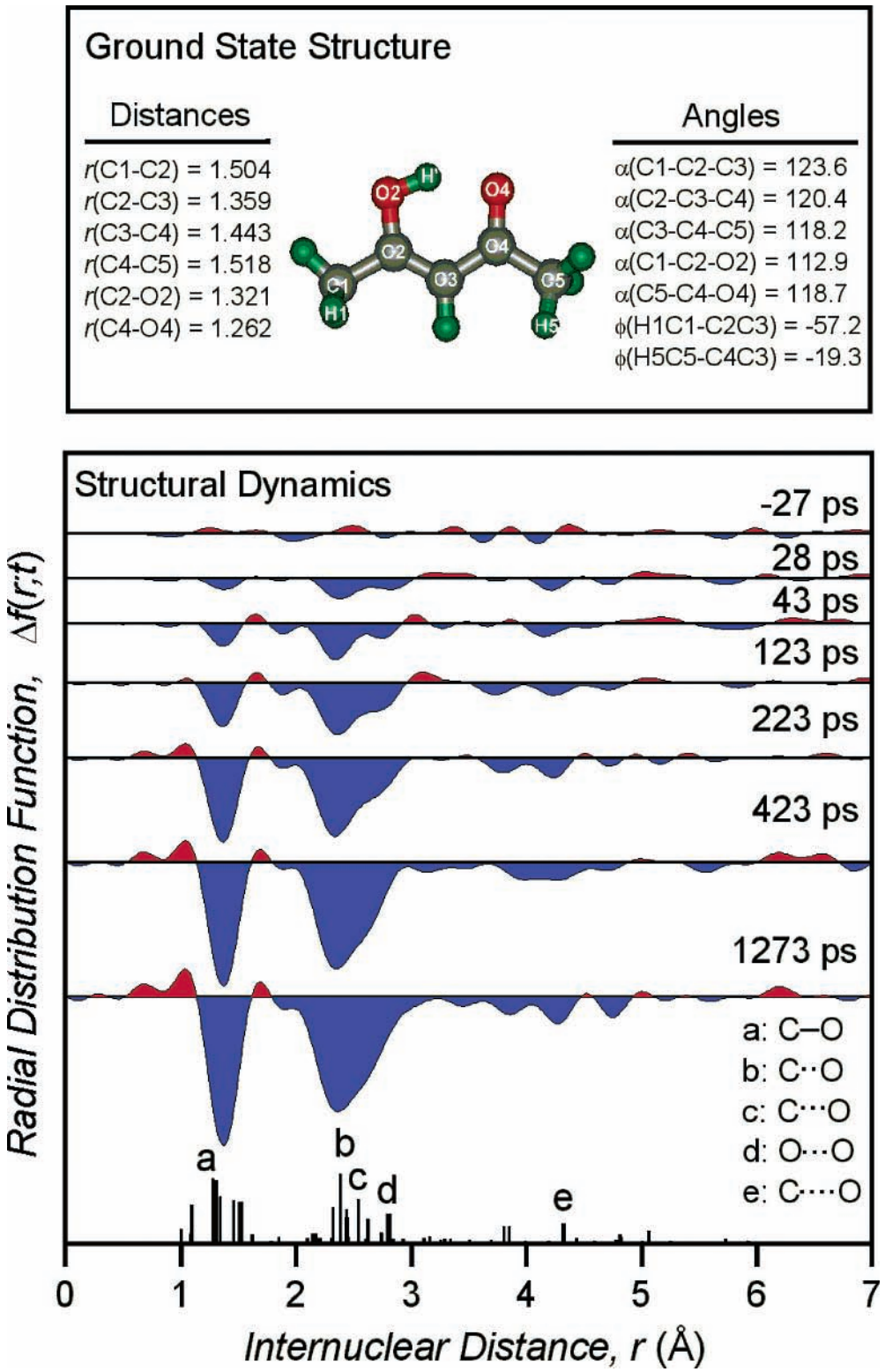

Figure 1. Ground-state structure of enolic acetylacetone (top) and structural dynamics observed (bottom). Shown are the time-resolved radial distribution curves, $\Delta f(r;t)$. The blue highlighted regions represent net depletion of internuclear pairs ("old bonds"). Red highlighting represents the formation of new distances. The vertical lines at the bottom indicate their relative contributions; proportional to nZ_iZ_j/r_{ij} (Z is the atomic number and r is the internuclear distance). Distances are in angstroms and angles are in degrees.

the interaction region. Diffracted electrons were collected by a low-noise CCD camera.

The molecular sample was introduced into the chamber through a nozzle maintained at 155 °C. Acetylacetone (2,4-pentanedione) was purchased from Aldrich (>99.0%) and degassed before use by three cycles of the freeze−pump−thaw procedure.

The starting geometries for structural analysis were obtained by quantum chemical (DFT) calculations at the B3LYP/6-311G(d,p) level. Structural refinement was conducted with Monte Carlo sampling and least-squares fitting incorporated into home-built analysis software. Theoretical models were quantitatively rated by their R values, a typical statistical measure used in electron diffraction.[17]

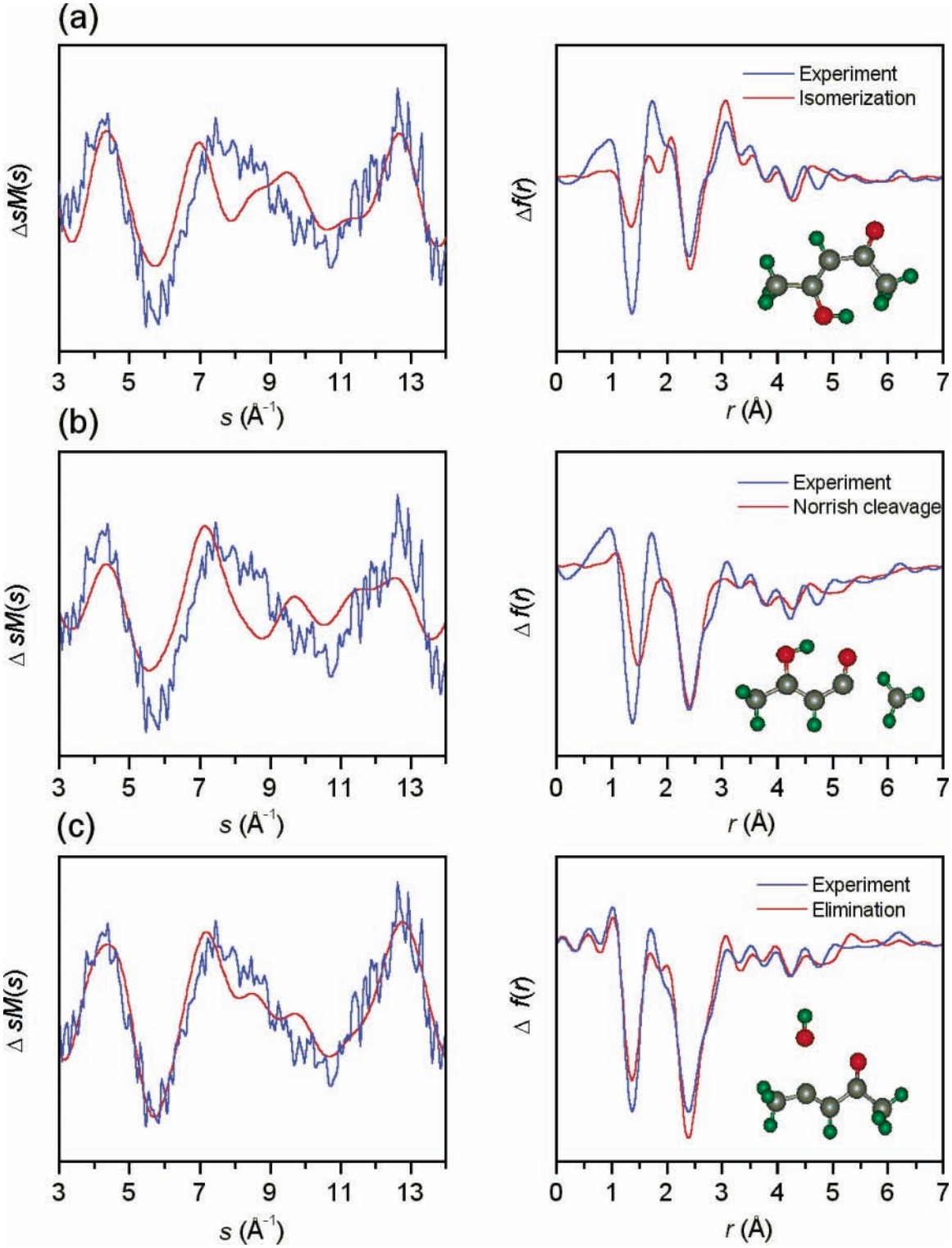

Figure 2. Experimental and theoretical diffraction-difference data ($\Delta sM(s)$ and $\Delta f(r)$; +1273 ps (reference = −77 ps)) for different pathways. (a) Isomerization to *cis-trans-cis* enol; $R = 1.103$. (b) Norrish Type-I cleavage of the methyl group; $R = 1.222$. (c) Loss of the OH radical; $R = 0.533$. The minor difference in appearance of the experimental data is an effect of different background curves. The polynomial background is calculated and subtracted from the data to best accommodate each theoretical model.

III. Results and Discussion

Two-dimensional time-resolved diffraction frames were collected for a range of time delays from −77 to +1273 ps with respect to the arrival of the initiating laser pulse. Frames recorded at each time point were converted to the modified molecular scattering curves, $sM(s)$, for electron diffraction structural analysis. The radial distribution curves, $f(r)$, were obtained by Fourier transform of the $sM(s)$ curves. Frames obtained before time-zero contain information only on the ground-state structure of AcAc. Figure 1 (top) shows the refined ground-state structure of the enol tautomer. Single and double bonds are clearly defined, demonstrating the asymmetry of the molecule and the contribution of some electron delocalization.[3]

For the time-resolved diffraction analysis, the ground-state data before time-zero was used as a reference and differenced from post-time-zero data to create difference curves, $\Delta sM(s)$

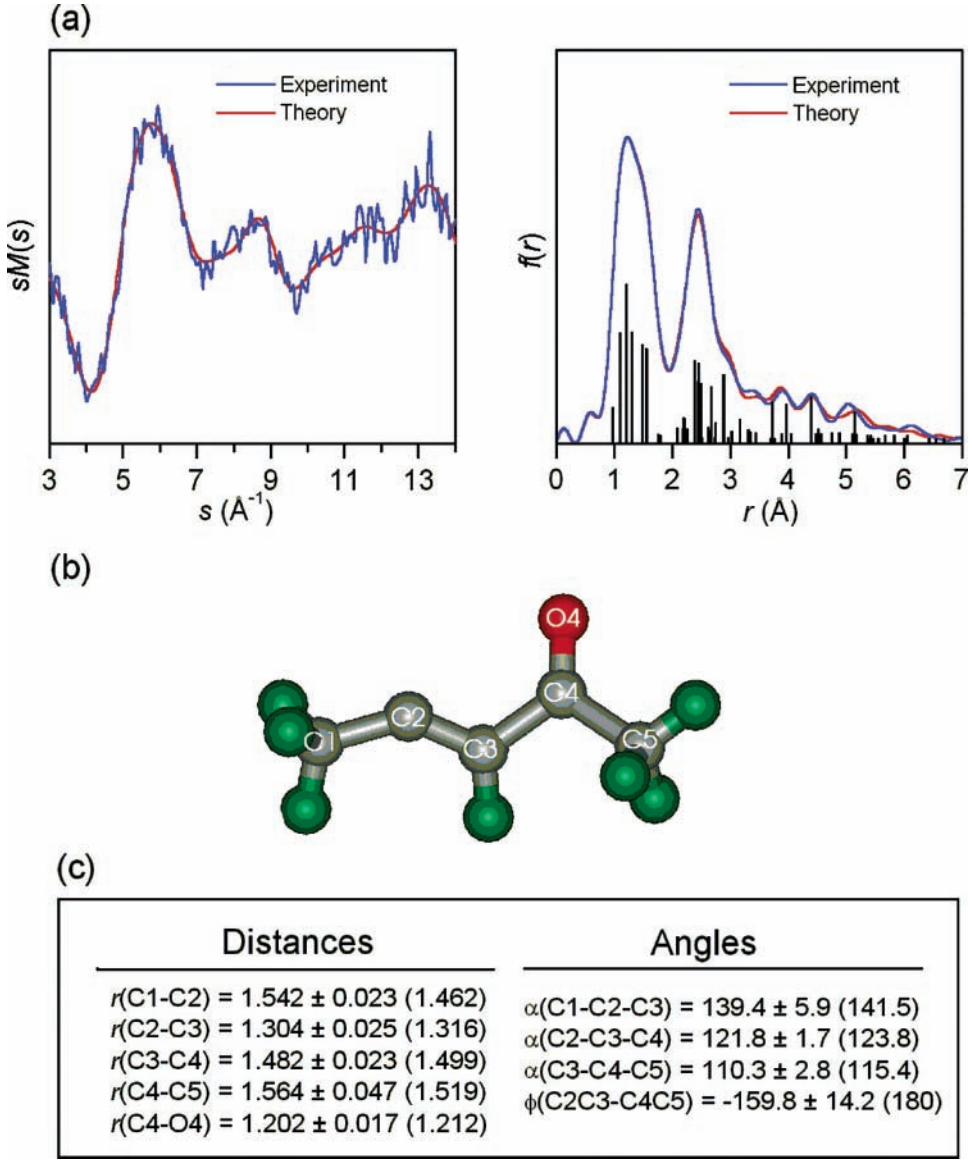

Figure 3. (a) Refined theoretical $sM(s)$ and $f(r)$ curves and the +1273 ps "product only" data; $R = 0.273$. The bars below $f(r)$ show the intensity contributed by each internuclear separation in the molecule; proportional to nZ_iZ_j/r_{ij}. In "product-only" format the fitted parent contribution to the reaction is added to the difference data, leaving only the product signal. (b) Refined structure of the 2-penten-4-on-3-yl radical. (c) Refined parameters of the fitted structure compared with starting values obtained by DFT (in parentheses). Distances are in angstroms and angles are in degrees.

and $\Delta f(r)$, thereby obtaining the net structural change from reactants to products.[13] Figure 1 (bottom) shows the time-resolved difference radial distribution curves using −77 ps as the reference. The curves clearly map out the reaction − the time-dependent depletion of old bonds and formation of new bonds.

To reveal the reaction pathway(s), the experimental $\Delta sM(s)$ and $\Delta f(r)$ curves at the +1273 ps delay (reference = −77 ps) are compared with theoretical $\Delta sM(s)$ and $\Delta f(r)$ curves of several reaction channels: isomerization, Norrish cleavage, and elimination, as shown in Figure 2. This visual comparison provides an intuitive way of choosing an appropriate starting point for structural refinement. Although some isomerization of the chelated (H-bond intact) enol into nonchelated enol in matrices[6−8] and in solution[9] has been studied, the poor match ($R = 1.103$) between this model and the data (see Figure 2a) indicates that the pathway is not significant in the isolated reaction; the experimental $\Delta f(r)$ shows high-amplitude peaks corresponding to bond scission that are not provided by the theoretical model. Norrish Type-I reactions, such as the loss of the acetyl or methyl groups were considered and discarded as poor models for the data (see Figure 2b). This is consistent with the structural dynamics discussed below.

The tautomerization channel, i.e., formation of keto and enol tautomers after internal conversion to the "hot" ground-state, also studied by spectroscopy in matrices,[7] appeared to fit the data ($R = 0.508$; not shown) when utilizing quantum chemically determined structures. A mixture of the structures of both keto and enol tautomers in their ground states at 2256 K was used.[18] AcAc with this internal energy will consist of enol and keto tautomers in a 1:2 ratio. Structural refinement for this channel did not greatly improve the quality of the fit. Moreover, fitting the fractions of keto and enol tautomers eliminated the enol contribution completely, in contradiction to the thermodynamics of population distribution.

Superior structural refinement results were obtained with the use of the OH loss model ($R = 0.533$, see Figure 2c). OH loss has been observed by laser-induced fluorescence (LIF) spectroscopy of gas-phase AcAc.[10−12] In our UED study, combinations of the previously mentioned channels were tested by

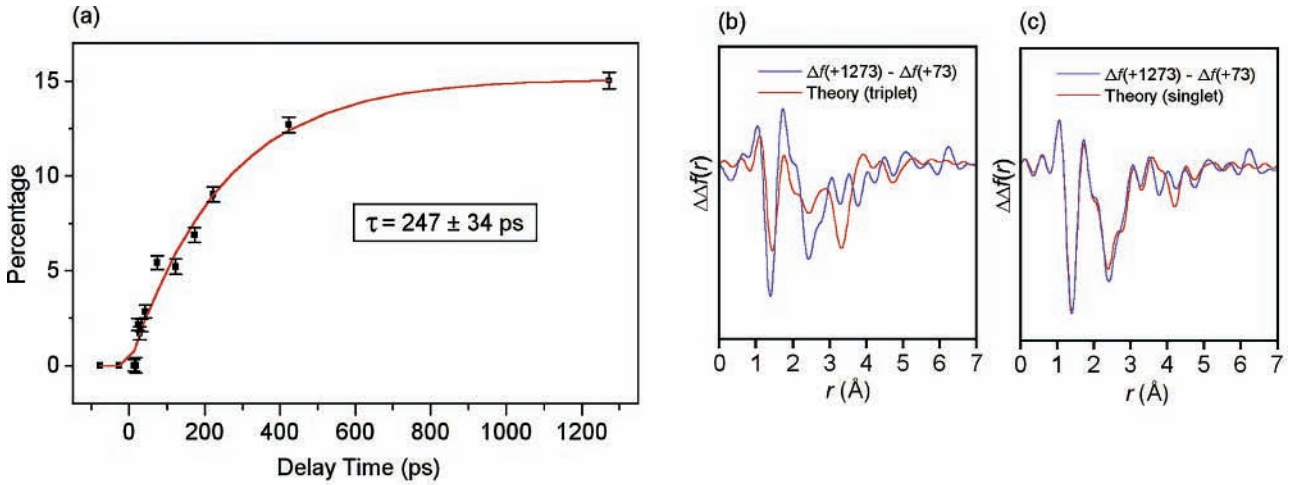

Figure 4. (a) Percentage of the OH-loss products for all experimental time points, showing a rise time of 247 ± 34 ps. (b) Difference-difference data, +1273 ps frame − reference frame (+73 ps), and the theoretical model corresponding to T_1(DFT) → OH-loss products. (c) Difference-difference data, +1273 ps frame − reference frame (+73 ps), and the theoretical model corresponding to S → OH-loss products. S is an approximation of the singlet manifold structure made using a combination of S_1 and S_2 geometries (CASSCF) in ~1:3 ratio. (See text.)

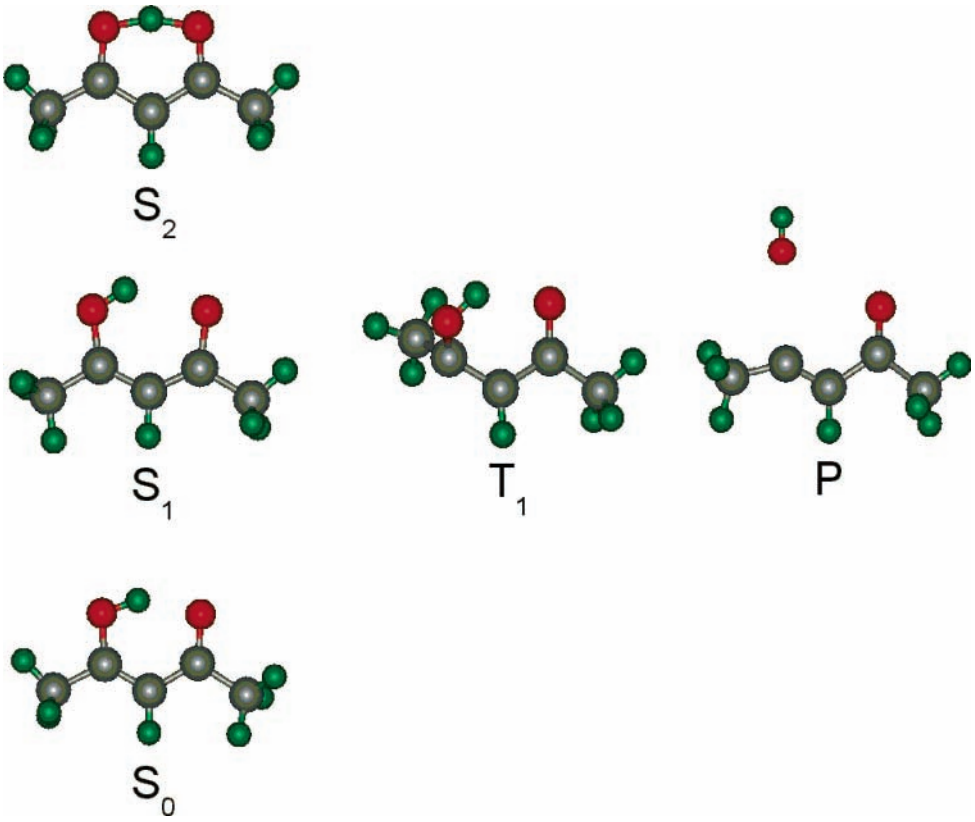

Figure 5. Structures involved in the dynamics of the OH elimination reaction. Ground-state (S_0) and OH elimination product (P) structures were experimentally obtained using UED (see text). Excited-state structures (S_1, S_2, T_1) were obtained by *ab initio* methods at the CASSCF(10,9)/6-31G(d,p) level.

comparing the data with mixtures of several theoretical models. This produced slightly improved fits (as more degrees of freedom are present). However, since the OH loss channel always remained the dominant component, structural refinement was carried out with this channel being the reaction pathway.

Having identified the reaction channel, the structure of its corresponding product, the 3-penten-2-on-4-yl radical, was then refined. The final refined structure is shown in Figure 3 (R = 0.338). The refined covalent bond distances and angles show some deviations from the equilibrium structures predicted by quantum chemical calculations. The bonds connecting the methyl groups to the remainder of the carbon skeleton, r(C1−C2) and r(C4−C5), are longer by 0.080 and 0.045 Å, respectively. Also at variance from theory, the acetyl group is rotated out of the plane of the molecule by ~20° instead of being coplanar. This indicates that the radical is able to rotate around the C−C single bond. The fitted value reflects an average over all the rotations present in the product.

Structurally, due to the loss of intramolecular hydrogen bonding, the resonance of the conjugated system is disrupted and the bonds revert to a more unperturbed state. The skeletal distances in the ground-state enol, r(C2−C3) = 1.359 Å, r(C3−C4) = 1.443 Å, and r(C4−O4) = 1.262 Å,[3] become 1.304 ± 0.025 Å, 1.482 ± 0.023 Å, and 1.202 ± 0.017 Å, respectively,

in the product radical where the hydrogen bond is severed and resonance stabilization is lost. Mean amplitudes of vibration were deduced to be consistent with a somewhat cold structure in agreement with a previous finding[12] that a significant fraction of internal energy is released into translational motion of the fragments (note that our initial thermal energy is higher than the temperature of the supersonic expansion[12]).

Using the refined product structure shown in Figure 3, its fractional contribution to each of the other time points was obtained. The plot of the product fraction versus time is shown in Figure 4a. Over the entire time scale, a time constant of 247 ± 34 ps was obtained from nonlinear fitting using a first-order reaction model. To test the validity of a direct first-order reaction (without intermediates), new diffraction-difference data were obtained by using a frame after time-zero as the reference. These alternative difference data (referred to hereafter as $\Delta\Delta sM(s)$ or difference-difference data) are shown in Figure 4b,c for the +1273 ps frame with the +73 ps frame as the reference. In a first-order reaction, the resulting data would be lower in amplitude yet still correspond to the parent-to-product reaction scheme. Conversely, if the reaction has multiple steps, the entire parent contribution will be removed in the difference-difference data. These data will then contain information on the intermediate-to-product reaction. The data shown in Figure 4b,c suggests the latter case and the presence of an intermediate structure.

Elimination of OH from the T_1 ($\pi\pi^*$) state of AcAc has been suggested in the literature.[12] The possibility of the T_1 structure as the intermediate is tested by comparing theoretical $\Delta\Delta sM(s)$ and $\Delta\Delta f(r)$ with experimental data (see Figure 4b). The T_1 state possesses a nonplanar structure with the C−O moiety twisted 66° out of the skeletal plane resulting in internuclear distances drastically different from S_0; for example, the O···O separation is 3.426 Å for the T_1 structure, compared to 2.592 Å for the S_0 structure.[3] The T_1 structure does not fit the experimental $\Delta\Delta sM(s)$ as the intermediate, ruling out a slow dissociation from T_1 as the rate determining step of the reaction. Figure 4c suggests that the intermediate structure is of singlet character, manifested as a combination of S_1 and S_2 structures because of their proximity in energy.[19] Furthermore, the structureless absorption band[4,5,11] and absence of fluorescence[10,12] suggest that the S_2 state is very short-lived. Consequently, the observed rise is the rate determining step, the intersystem crossing (ISC) from S_1 to T_1; this long lifetime of S_1 has also been observed for malonaldehyde.[20] The appearance of pseudo-first-order behavior is consistent with ISC as the rate-determining step for the overall elimination reaction.

Structural dynamics can now be related to the reaction pathway(s) involving different electronic states. The transition from S_2 to S_1 is ultrafast (fluorescence was not observed[10,12]), as discussed above. In the S_1 ($n\pi^*$) state, the structure is planar and the lifetime of molecules in this state is determined by the ISC to the T_1 ($\pi\pi^*$) state. The structure in the T_1 state is nonplanar (C−O moiety twisted 66° out of the skeletal plane), and as such it promotes the cleavage of the OH radical in order to reform the double bond present in the final radical. It is now easy to understand why the dominant reaction channel is not a Norrish-type cleavage as would be prompted by a T_1 structure of $n\pi^*$ excitation. The structures involved in the dynamics of this elimination are pictured in Figure 5.

IV. Conclusion

The sensitivity of UED to all nuclear positions reveals that the ground state of AcAc is of C_s asymmetric structure. The OH loss is the dominant channel after 266 nm excitation, but transient structures are found to precede the final product. The overall time constant for OH formation is determined to be 247 ± 34 ps. The influence of resonance stabilization on the molecular structure of the ground state[3] is lost in the T_1 state and the OH moiety is no longer coplanar with the conjugated bonds, aiding in efficient OH elimination. The $\pi\pi^*$ nature of this structure facilitates reaction pathways that are not typical among ketones − OH-elimination from the β carbon as opposed to a Norrish Type-I cleavage. The absence of resonance stabilization results in the more "electron-localized" structure of the 3-penten-2-on-4-yl radical, and the change in bond distances is directly observed. With ultrafast electron diffraction it was possible to map out changes of structures with time on the energy/state landscape of the reaction.

Acknowledgment. This work was supported by the National Science Foundation and in part by the Air Force Office of Scientific Research. S.T.P. gratefully acknowledges the partial support provided by the Post-doctoral Fellowship Program of the Korean Science & Engineering Foundation (KOSEF).

References and Notes

(1) Perrin, C. L.; Nielson, J. B. *Annu. Rev. Phys. Chem.* **1997**, *48*, 511.

(2) Gilli, G.; Bellucci, F.; Ferretti, V.; Bertolasi, V. *J. Am. Chem. Soc.* **1989**, *111*, 1023.

(3) Srinivasan, R.; Feenstra, J. S.; Park, S. T.; Xu, S.; Zewail, A. H. *J. Am. Chem. Soc.* **2004**, *126*, 2266.

(4) Nakanishi, H.; Morita, H.; Nagakura, S. *Bull. Chem. Soc. Jpn.* **1977**, *50*, 2255.

(5) Walzl, K. N.; Xavier, I. M., Jr.; Kuppermann, A. *J. Chem. Phys.* **1987**, *86*, 6701.

(6) Roubin, P.; Chiavassa, T.; Verlaque, P.; Pizzala, L.; Bodot, H. *Chem. Phys. Lett.* **1990**, *175*, 655.

(7) Nagashima, N.; Kudoh, S.; Takayanagi, M.; Nakata, M. *J. Phys. Chem. A* **2001**, *105*, 10832.

(8) Coussan, S.; Manca, C.; Ferro, Y.; Roubin, P. *Chem. Phys. Lett.* **2003**, *370*, 118.

(9) Veierov, D.; Bercovici, T.; Fischer, E.; Mazur, Y.; Yogev, A. *J. Am. Chem. Soc.* **1977**, *99*, 2723.

(10) Yoon, M.-C.; Choi, Y. S.; Kim, S. K. *J. Chem. Phys.* **1999**, *110*, 11850.

(11) Yoon, M.-C.; Choi, Y. S.; Kim, S. K. *Chem. Phys. Lett.* **1999**, *300*, 207.

(12) Upadhyaya, H. P.; Kumar, A.; Naik, P. D. *J. Chem. Phys.* **2003**, *118*, 2590.

(13) Srinivasan, R.; Lobastov, V. A.; Ruan, C.-Y.; Zewail, A. H. *Helv. Chim. Acta* **2003**, *86*, 1763, and references therein.

(14) Ihee, H.; Lobastov, V. A.; Gomez, U. M.; Goodson, B. M.; Srinivasan, R.; Ruan, C.-Y.; Zewail, A. H. *Science* **2001**, *291*, 458.

(15) Lobastov, V. A.; Srinivasan, R.; Vigliotti, F.; Ruan, C.-Y.; Feenstra, J. S.; Chen, S.; Park, S. T.; Xu, S.; Zewail, A. H. In *Ultrafast Optics IV, Springer Series in Optical Sciences*; Krausz, F., Korn, G., Corkum, P., Walmsley, I., Eds.; Springer-Verlag: Berlin, 2003; p 413.

(16) Ruan, C.-Y.; Vigliotti, F.; Lobastov, V. A.; Chen, S.; Zewail, A. H. *Proc. Natl. Acad. Sci. U.S.A.* **2004**, *101*, 1123.

(17) Hargittai, I.; Hargittai, M. *Stereochemical Applications of Gas-phase Electron Diffraction. Part A. The Electron Diffraction Technique.*; VCH: New York, 1988.

(18) This temperature was calculated considering a statistical distribution of the absorbed energy of a single photon among all modes in the ground state.

(19) Lim, E. C. *J. Phys. Chem.* **1986**, *90*, 6770.

(20) Arias, A. A.; Wasserman, T. A. W.; Vaccaro, P. H. *J. Chem. Phys.* **1997**, *107*, 5617.